Available online at www.sciencedirect.com

ScienceDirect

Mendeleev Commun., 2019, **29**, 279–281

Mendeleev Communications

Influence of synthesis temperature on structural and magnetic properties of magnetoferritin

Lucia Balejčíková,*[a,b] Jozef Kováč,[b] Vasil M. Garamus,[c] Mikhail V. Avdeev,[d] Viktor I. Petrenko,[d,e] László Almásy[f,g] and Peter Kopčanský[b]

[a] *Institute of Hydrology, Slovak Academy of Sciences, 841 04 Bratislava, Slovakia. E-mail: balejcikova@saske.sk*
[b] *Institute of Experimental Physics, Slovak Academy of Sciences, 040 01 Košice, Slovakia*
[c] *Helmholtz-Zentrum Geesthacht, Centre for Materials and Coastal Research, 21502 Geesthacht, Germany*
[d] *Joint Institute for Nuclear Research, 141980 Dubna, Moscow Region, Russian Federation*
[e] *Taras Shevchenko National University of Kyiv, 01033 Kyiv, Ukraine*
[f] *State Key Laboratory of Environment-Friendly Energy Materials, Southwest University of Science and Technology, 621010 Mianyang, China*
[g] *Institute for Solid State Physics and Optics, Wigner Research Centre for Physics, Hungarian Academy of Sciences, H-1525, Budapest POB 49, Hungary*

DOI: 10.1016/j.mencom.2019.05.012

The variation of synthesis temperature made it possible to produce artificial ferritins possessing different structural and magnetic properties, size distribution, and colloidal stability. The effect of synthesis temperature on the core structure and stability of protein shell was investigated using small-angle neutron scattering, small-angle X-ray scattering, SQUID magnetometry, dynamic light scattering, and zeta potential measurements. The optimal temperature was established for the synthesis of artificial ferritin suitable for biomedical imaging applications at ~60 °C, which is close to the protein denaturation temperature.

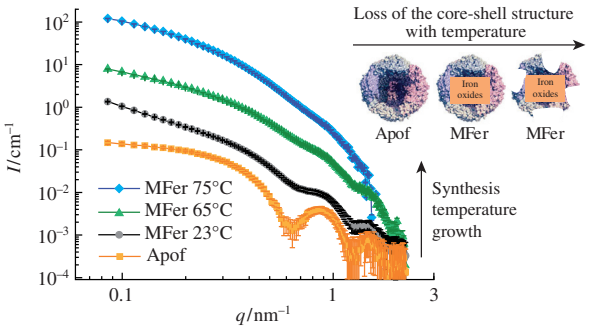

Iron is one of the essential elements for living organisms. However, an excess of its ions is toxic, and therefore, they are stored in the cavity of a spherical protein, so-called ferritin. Ferritin shapes as a hollow spherical shell with an external diameter of 12 nm and thickness of 2 nm. Functional ferritin, according to the specific requirements of each organism, could bind up to 4500 iron atoms arranged in a crystal structure similar to that of ferrihydrite mineral.[1] It was shown that the empty ferritin structure (apoferritin) can also be used for the chemical synthesis of other types of mineral cores composed of various metal ions (Cu^{2+}, Mn^{2+}, *etc.*).[2,3] Under specific physicochemical conditions, it is possible to prepare artificial ferritin with unique superparamagnetic properties, *i.e.* magnetoferritin (MFer), which can be useful in various biomedical applications (*e.g.*, a contrast agent in radiology, a drug carrier in targeted transport, or a standard in diagnostics of various diseases).[4,5] The MFer synthesis protocol was derived from the general scheme of preparation of pure magnetic nanoparticles, which is based on the co-precipitation of Fe^{2+} and Fe^{3+} salts at a high temperature (50–80 °C) under alkaline conditions (pH 8). The high thermal stability of apoferritin[6] makes this protein well suited for the synthesis of magnetic nanoparticles within its hollow core by a slow addition of Fe^{2+} ions followed by the controlled addition of oxidant under anaerobic conditions.[7] MFer was investigated using different physical methods such as magnetometry, electron microscopy, atomic force microscopy, Mössbauer spectroscopy, *etc.*[4,7,8] The latest results obtained by small-angle X-ray (SAXS) and neutron scattering (SANS)[9,10] revealed a partial destruction of the MFer protein shell with a loading factor (LF) above ~150 in comparison with a pure apoferritin shell (the LF is an average number of iron atoms per one protein biomacromolecule) as well as aggregation of MFer molecules and sedimentation of its solutions at LF > 600. This degradation is most probably caused by iron binding or a formation of a magnetic core inside the protein shell.[9–11] To understand the protein shell destruction, the influence of pH was studied using SAXS.[12] The highest stability of MFer biomacromolecule was observed at pH 7–9, while the protein shell was decomposed at pH below 6.[12] This means that pH in the synthesis process did not affect the shell stability. The exact reason of the degradation after synthesis has not been fully understood, and in particular, the effect of synthesis temperature on the chemical composition and magnetic properties of the inorganic core as well as on the structure of the protein shell has not been investigated.

This work shows that synthesis temperature plays a crucial role in the development of the protein shell structure *in vitro*, iron binding, and magnetic character of magnetoferritin. Using small-angle scattering techniques, we observed a significant influence of the synthesis temperature on the structure of MFer proteins prepared with a similar amount of embedded iron oxide.

The DLS measurements revealed the variation of the average hydrodynamic diameter ($\langle D_{HYDR} \rangle$) of the nanoparticles as a function of LF and synthesis temperature (Figure S1, Online Supplementary Materials) in comparison with the pure apoferritin (12 nm). Higher LF (640–940) were characterized by a higher $\langle D_{HYDR} \rangle$ value. This effect was also observed in our previous works[9,10] and points to the impact of LF on the structure and

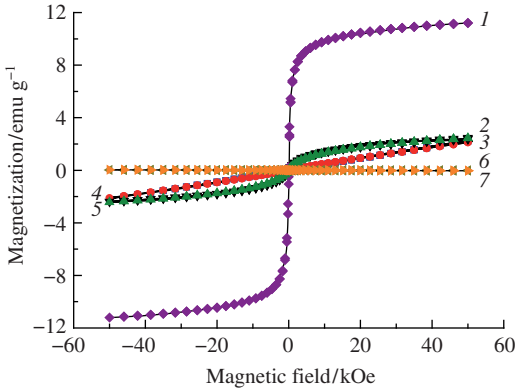

Figure 1 Room temperature magnetization curves of MFer samples prepared at various synthesis temperatures with different loading factors in comparison with apoferritins: (*1*) MFer with LF 940 prepared at 75 °C, (*2*) MFer with LF 660 prepared at 65 °C, (*3*) MFer with LF 810 prepared at 55 °C, (*4*) MFer with LF 640 prepared at 37 °C, (*5*) MFer with LF 730 prepared at 23 °C, (*6*) apoferritin heated at 65 °C for 100 min, and (*7*) pure apoferritin solution.

stability of MFer solutions. It was shown that synthesis temperature affects the size of nanoparticles. A similar effect can be detected when comparing pure apoferritin with that heated at 65 °C for 100 min. Zeta potentials of all samples were negative and varied between –22 and –29 mV, indicating that all the samples exhibit sufficient colloidal stability (see Figure S1).

Magnetic measurements of artificial ferritins revealed the superparamagnetic behavior of their nanoparticles (Figure 1). While samples with lower LF and synthesis temperature exhibited relatively weak magnetization, the curve for the highest LF prepared at 75 °C showed the saturation of about 14 emu g^{-1} (see Figure 1). We assume that the reason for this difference is related to the formation of nano-sized magnetite/maghemite nanocrystals.[8] At lower synthesis temperatures, predominantly ferrihydrite-like minerals were formed similar to those in native ferritin.[13]

SANS curves of freeze dried MFer samples dissolved in D_2O with a protein concentration of 6 mg ml^{-1} and prepared with high iron loading at different synthesis temperatures are shown in Figure 2. Scattering maxima and minima characteristic of core-shell structure type were observed for MFer with the synthesis temperature in the range of 23–37 °C. The particle aggregation at a typical q-range below 0.2 nm^{-1} is probably associated with a strong iron binding as was reported previously.[9,10] In this case, the effect of the synthesis temperature on the MFer structure is masked by the strong aggregation. The SANS curves for MFer with higher LFs (640–940) synthesized in the range from 23

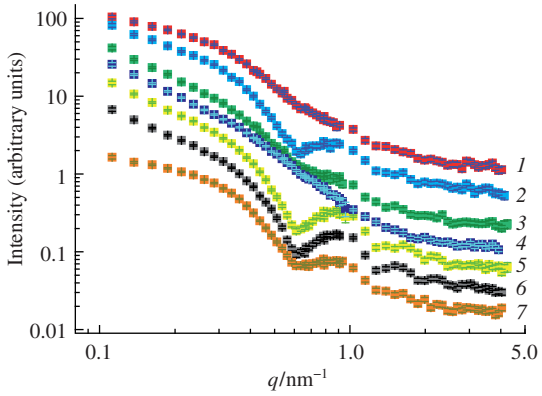

Figure 2 SANS curves of MFer samples prepared at various synthesis temperatures with different loading factors in comparison with apoferritin: (*1*) apoferritin heated at 65 °C for 100 min, (*2*) MFer with LF 940 prepared at 75 °C, (*3*) MFer with LF 660 prepared at 65 °C, (*4*) MFer with LF 810 prepared at 55 °C, (*5*) MFer with LF 640 prepared at 37 °C, (*6*) MFer with LF 730 prepared at 23 °C, and (*7*) pure apoferritin solution.

to 75 °C, demonstrate a loss of the core-shell structure upon increasing the synthesis temperature and rising LF, respectively. Despite relatively high LF of 730 and 640, the core-shell structure of MFer was preserved only at the synthesis temperatures of 23 and 37 °C. In the case of synthesis temperatures of 55 °C (LF 810) and 65 °C (LF 660), the LF effect was stronger than the effect of synthesis temperature. The increase in the scattering intensity at $q < 0.7$ nm^{-1} for all the mentioned samples shows a fraction of aggregated particles. The impact of the highest synthesis temperature 75 °C (near the protein denaturation temperature limit,[6] ~80 °C) was masked by the effect of the high LF 940, which was observed in our previous work[10] for high LFs, *i.e.*, the formation of large aggregated nanoparticles that sedimented before the SANS measurements. Therefore, the SANS data of this sample are similar to those for the pure apoferritin. The undeniable effect of the synthesis temperature was revealed when comparing the scattering from pure apoferritin diluted in AMPSO buffer at room temperature with the same apoferritin heated at 65 °C for 100 min. It should be noted that magnetite/maghemite in the protein cavity will not be formed without high-temperature treatment, and without magnetite/maghemite, the magnetic susceptibility of MFer will be very low. The mechanisms of iron core formation in magnetoferritin include the mineralization of iron oxides inside apoferritin shell using controlled thermal oxidation conditions. This process could be similar to the formation of an inorganic nucleus in physiological ferritin[14] and can be summarized in four main steps: Fe^{2+} ions input, Fe^{2+} oxidation to Fe^{3+}, nucleation, and growth of inorganic nucleus.[15]

It was confirmed that the iron accumulation and presence of magnetite crystals in pathological ferritin could be the reason of development of various diseases.[16,17] In recent years, a great emphasis has been put on the early diagnostics of those diseases using various techniques such as magneto-optical or magnetic resonance imaging (MRI) measurements. Magnetoferritin prepared under extreme conditions such as high temperature, which insure formation of magnetite/maghemite nanoparticles, and high LF should increase the hypointensive artefacts in MRI. Such findings are highly promising for exploiting magnetoferritin as a non-invasive diagnostics tool of pathological processes, where the magnetoferritin particles could be utilized as MRI iron quantification standards.[18–22]

SAXS experiments were performed on samples prepared with lower LF (270–280). At such loadings, the oscillations of the scattering form-factor are more pronounced, the particle agglomeration is relatively weak, and the scattering from the magnetic nanoparticles is also weak. Therefore, the effect of the synthesis temperature on the MFer structure can be observed more clearly. Indeed, Figure 3 shows a gradual smoothing of the scattering curves with an increase in the synthesis temperature, indicating the decomposition of the core-shell structure of apoferritin with raising the preparation temperature.

Such synthesis temperature dependent variation of the core-shell structure has never been previously studied for the magnetoferritin. It is generally known that the protein undergoes structural changes under the influence of temperature, while the most significant changes occur at the denaturation limit, where the protein loses its functionality and the spatial arrangement of the peptide chain. Similar variations in the magnetoferritin structure under the influence of different loading factors[9–11] and pH[12] have been previously observed. The acquired data make it possible to conclude that the synthesis temperature plays a crucial role in the formation of the protein structure and magnetic properties, and this has to be taken into account for future applications of magnetoferritin in biomedical imaging.

In conclusion, we have observed structural differences in the protein shell integrity and a change of the magnetic properties of

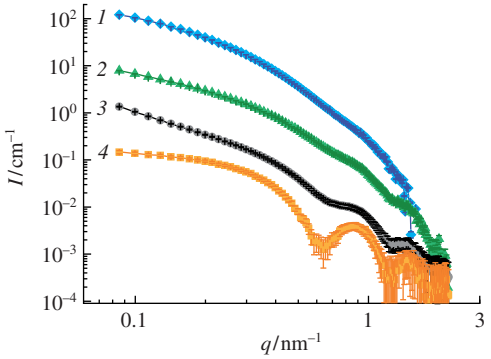

Figure 3 SAXS curves for MFer samples with similar LF prepared at different temperatures in comparison with pure apoferritin: (*1*) MFer with LF 270 prepared at 75 °C, (*2*) MFer with LF 270 prepared at 65 °C, (3) MFer with LF 280 prepared at 23 °C, and (*4*) pure apoferritin.

MFer metallic core as a function of the synthesis temperature. Besides revealing the formation mechanism for the magnetic core, our data suggested a way to optimize the synthesis process, *i.e.*, to achieve better structural stability and higher magnetization of the material. Our results have demonstrated that low synthesis temperatures lead to the formation of stable core-shell structures, while higher temperatures provide samples with a higher magnetization. Therefore, for obtaining good structural and magnetic properties, a compromise should be found. The present results indicate that the optimal temperature for the MFer synthesis is between 55 and 65 °C, and the LF is below 600. Magnetoferritin with higher magnetization should be prepared at high LF (above 600) at the temperatures close to the protein denaturation point. These conditions ensure favorable physical properties, *i.e.* strong contrast and sufficient colloidal stability, suitable for biomedical imaging applications.

This work was supported by the Slovak Scientific Grant Agency VEGA (project nos. 2/0016/17 and 2/0062/16), the Slovak Research and Development Agency (contract no. APVV-015-0453), the Agency of the Ministry of Education, Science, Research, and Sport of the Slovak Republic for the Structural Funds of EU (project nos. 26210120012 and 26220220186), and by the MAGBBRIS project Euronanomed III.

Online Supplementary Materials

Supplementary data associated with this article can be found in the online version at doi: 10.1016/j.mencom.2019.05.012.

References

1 G. Jutz, P. van Rijn, B. Santos Miranda and A. Böker, *Chem. Rev.*, 2015, **115**, 1653.
2 F. C. Meldrum, T. Douglas, S. Levi, P. Arosio and S. Mann, *J. Inorg. Biochem.*, 1995, **58**, 59.
3 T. Douglas and V. T. Stark, *Inorg. Chem.*, 2000, **39**, 1828.
4 F. C. Meldrum, B. R. Heywood and S. Mann, *Science*, 1992, **257**, 522.
5 E. C. Theil, R. K. Behera and T. Tosha, *Coord. Chem. Rev.*, 2013, **257**, 579.
6 S. Stefanini, S. Cavallo, C. Q. Wang, P. Tataseo, P. Vecchini, A. Giartosio and E. Chiancone, *Arch. Biochem. Biophys.*, 1996, **325**, 58.
7 K. K. W. Wong, T. Douglas, S. Gider, D. D. Awschalom and S. Mann, *Chem. Mater.*, 1998, **10**, 279.
8 M. J. Martínez-Pérez, R. de Miguel, C. Carbonera, M. Martínez-Júlvez, A. Lostao, C. Piquer, C. Gómez-Moreno, J. Bartolomé and F. Luis, *Nanotechnology*, 2010, **21**, 465707.
9 L. Melníková, V. I. Petrenko, M. V. Avdeev, V. M. Garamus, L. Almásy, O. I. Ivankov, L. A. Bulavin, Z. Mitróová and P. Kopčanský, *Colloids Surf., B*, 2014, **123**, 82.
10 L. Melnikova, V. I. Petrenko, M. V. Avdeev, O. I. Ivankov, L. A. Bulavin, V. M. Garamus, L. Almásy, Z. Mitroova and P. Kopcansky, *J. Magn. Magn. Mater.*, 2015, **377**, 77.
11 L. Melníková, Z. Mitróová, M. Timko, J. Kováč, M. V. Avdeev, V. I. Petrenko, V. M. Garamus, L. Almásy and P. Kopčanský, *Mendeleev Commun.*, 2014, **24**, 80.
12 L. Balejčíková, V. M. Garamus, M. V. Avdeev, V. I. Petrenko, L. Almásy and P. Kopčanský, *Colloids Surf., B*, 2017, **156**, 375.
13 J. M. Cowley, D. E. Janney, R. C. Gerkin and P. R. Buseck, *J. Struct. Biol.*, 2000, **131**, 210.
14 U. Testa, *Proteins of Iron Metabolism*, 1st edn., CRC Press, Atlanta, 2001.
15 A. M. Koorts and M. Viljoen, in *Acute Phase Proteins: Regulation and Functions of Acute Phase Proteins*, ed. F. Veas, IntechOpen, 2011, pp. 153–184.
16 M. A. Smith, P. L. R. Harris, L. M. Sayre and G. Perry, *Proc. Natl. Acad. Sci. USA*, 1997, **94**, 9866.
17 J. Dobson, *FEBS Lett.*, 2001, **496**, 1.
18 J. W. Bulte, T. Douglas, S. Mann, R. B. Frankel, B. M. Moskowitz, R. A. Brooks, C. D. Baumgarner, J. Vymazal and J. A. Frank, *Invest. Radiol.*, 1994, **29**, 214.
19 J. W. Bulte, T. Douglas, S. Mann, R. B. Frankel, B. M. Moskowitz, R. A. Brooks, C. D. Baumgarner, J. Vymazal, M. P. Strub and J. A. Frank, *J. Magn. Reson. Imaging*, 1994, **4**, 497.
20 V. C. Jordan, M. R. Caplan and K. M. Bennett, *Magn. Reson. Med.*, 2010, **64**, 1260.
21 Y. Zhao, M. Liang, X. Li, K. Fan, J. Xiao, Y. Li, H. Shi, F. Wang, H. S. Choi, D. Cheng and X. Yan, *ACS Nano*, 2016, **10**, 4184.
22 O. Strbak, L. Balejcikova, L. Baciak, J. Kovac, M. Masarova-Kozelova, A. Krafcik, D. Dobrota and P. Kopcansky, *J. Phys. D: Appl. Phys.*, 2017, **50**, 365401.

Received: 26th November 2018; Com. 18/5746